CA-3 | 23

ASAT

Military Technical College
CAIRO - EGYPT

DISTORTED FLOW IN A CURVED DUCT

M.M. Abdelrahman* and G.B. Salem**

ABSTRACT

This paper presents the numerical prediction for an inviscid, rotational and compressible flow in a two-dimensional curved duct with inlet total pressure distortion. The numerical method is a fully implicit finite difference technique solving the unsteady form of the continuity, Euler equations and the steady form of the energy equation. The results are presented for different cases of inlet total pressure distortion with the same average total pressure for all cases. These results are compared with those obtained from uniform inlet total pressure distribution to assess the deviation resulting from the uniform total pressure assumption.

*Assistant Professor, **Associate Professor,
Department of Aeronautical Engineering,
Faculty of Engineering, Cairo University, Guiza, Egypt.

Introduction

The motivation for selecting this geometry is that curved passages are extensively used in gas turbines, aircraft intakes and centrifugal pumps. In particular, this problem has become crucial to the successful development of new-generation of turbofans and turbojets. One of the major problems facing the engine designers is that of predicting the response of turbomachines to inlet flow nonuniformities resulting, e.g. from critical operation of the aircraft at the outer limits of the flight envelop or atmospheric turbulence or armament firing....etc. It is well known that axial compressors suffer a loss in performance and stability when the inlet flow is nonuniform and then can lead to engine surge which must be avoided at all events.

Due to the complexity of this problem, a great amount of numerical studies have been devoted to nonuniform flows in axial turbomachines either in the annular ducts extending in front of a compressor or in compressor blade passages which have a mild curvature. A brief description of these different numerical approaches can be found in Ref.[1-2].

This paper is devoted to the numerical investigation of the steady, adiabatic, two-dimensional, compressible, rotational, inviscid flow in a 90-deg curved duct with distorted inflow.

Numerical results are presented for six different cases of inlet total pressure distortion with a constant mean value for all cases. These cases are chosen to demonstrate the effect of inlet total pressure distortion on the behaviour of the flow in the duct.

6

Governing Equations

The method presented in this paper is based on the continuity, momentum and energy equations for inviscid, adiabatic, compressible and rotational flow. These basic equations are as follows

Continuity

$$\partial\rho/\partial t + \partial(\rho u)/\partial x + \partial(\rho v)/\partial y = 0 \qquad (1)$$

Momentum in x-direction

$$\partial(\rho u)/\partial t + \partial(p+\rho u^2)/\partial x + \partial(\rho uv)/\partial y = 0 \qquad (2)$$

Momentum in y-direction

$$\partial(\rho v)/\partial t + \partial(\rho uv)/\partial x + \partial(p+\rho v^2)/\partial y = 0 \qquad (3)$$

Energy

$$H = h + \tfrac{1}{2} V^2 = \text{const.} \qquad (4)$$

where ρ, p, u, v are the density, pressure and velocity components along x,y directions respectively. H is the total enthalpy.

Body Fitted Coordinate System

Curvilinear coordinates (η_1, $\eta 2$), as shown in Fig.1 , are used such that the discretised boundaries are coincident with the mesh points used in the numerical solution. The use of grid points coincident with the boundaries simplifies both the coding of the fluid flow

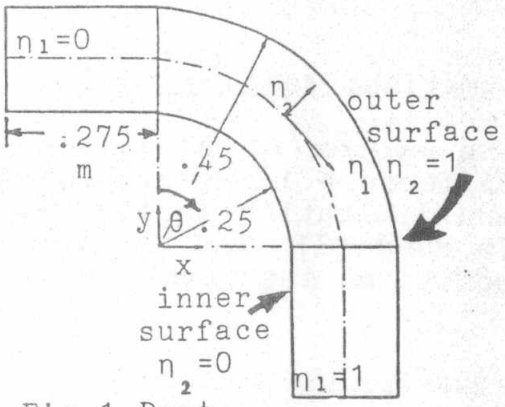

Fig.1 Duct geometry.

alogrithm and the application of the boundary conditions. The basic system of equations (1,2 and 3) take the following form in the curvilinear coordinate system

Continuity

$$\partial(\rho\sqrt{g})/\partial t + \partial(\rho v^1\sqrt{g})/\partial\eta_1 + \partial(\rho v^2\sqrt{g})/\partial\eta_2 = 0 \qquad (5)$$

Momentum in η_1 direction

$$\partial(\rho v^1\sqrt{g})/\partial t + \partial(\rho v^1 v^j\sqrt{g})/\partial\eta_j + g^{1j}\sqrt{g}\,\partial p/\partial\eta_j + \rho v^j v^k\sqrt{g}\,\tilde{a}^i{}_{jk} = 0 \qquad (6)$$

Momentum in η_2 direction

$$\partial(\rho v^2\sqrt{g})/\partial t + \partial(\rho v^2 v^j\sqrt{g})/\partial\eta_j + g^{2j}\sqrt{g}\,\partial p/\partial\eta_j + \rho v^j v^k\sqrt{g}\,\tilde{a}^i{}_{jk} = 0 \qquad (7)$$

where the terms with repeated indices are summed for j and k =1 to 2. The pressure is defined, using the energy eq. (4), by

$$p = \rho(H - \tfrac{1}{2} v^i v_i)\,(\acute{O}-1)/\acute{O} \qquad (8)$$

v_i and v^i are the covariant and contravariant velocity components in the η i direction. g is the determinant of the matrix $[g_{ij}]$. g_{ij} and g^{ij} are the covariant and the contravariant components of the metric tensor. $\tilde{a}^i{}_{jk}$ is the Christofell symbol.

Numerical Technique

The system of equations 5,6 and 7 is solved using a finite difference time-marching method. To avoid instability problem and limitation in time step Δt, a fully implicit time scheme is used [3]. The stability correction method is used as an ADI splitting sequence.

Boundary Conditions

Surface Boundaries. Slip condition is imposed along $\eta_2 = 0$ & $\eta_2 = 1$ for inner and outer surfaces by

$$V.\acute{A}^2 = v^2 = 0$$

where V is the velocity vector and $\acute{A}^2$ is the vector normal to η_2 = const.

Inlet Boundary. Two conditions are imposed namely
– The direction of the velocity ($v^2 = 0$)

- The total pessure P_o as a function of η_2

Outlet Boundary. Uniform static pressure is imposed.

Results and Discussions

The numerical solution of the governing equations is obtained in a 90-deg curved duct having a mean radius of curvature of 0.35 m , and is 0.2 m wide. At the inlet and the outlet, the curved duct is preceded and followed by 0.275 m straight sections of the same cross - sectional dimensions. The duct geometry and dimensions are given in Fig. 1.

The numerical computations were carried out on a micro-computer (IBM - Compatable) using a uniform (17x7) grid mesh in η_1 and η_2 directions, respectively.

Comparison with experimental data, for this geometry at low speeds was given in Ref.[4].

In this work, a uniform inlet total pressure distribution $\overline{P}_o$ (case 1) is compared with six different cases of inlet total pressure distortion (2a,2b,3a, 3b,4a and 4b) having the same average total pressure $\overline{P}_o$, as shown in Fig. 2. A uniform exit static pressure $p_e=0.9\ \overline{P}_o$ is considered for all cases.

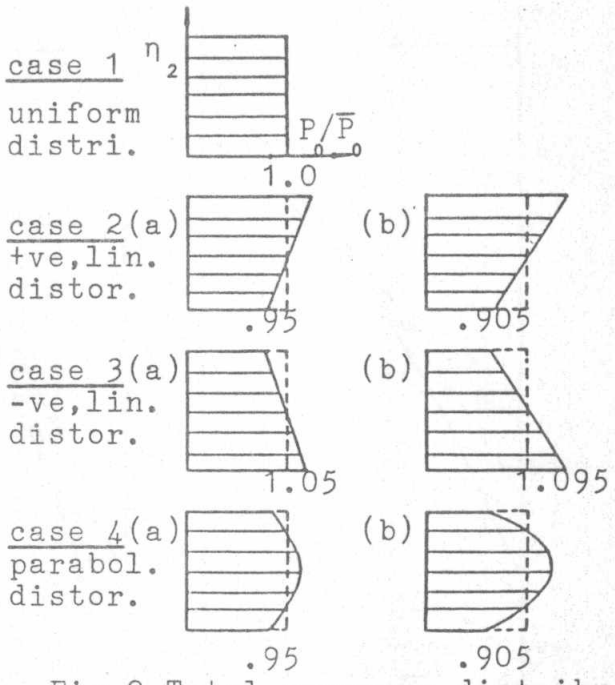

Fig.2 Total pressure distribution at inlet section.

Figure 3 shows the pressure distribution in radial direction at 0-,45- and 90-deg turning angles for cases 1,2,3 and 4. It can be noticed from these figures that the positive linear distortion (case 2) gives the higher pressure distribution while the negative linear distortion (case 3) gives the lower pressure distribution in comparison with that for case 1. However, the parabolic distortion (case 4) gives the lower pressure in the inner half and the higher distribution in the outer half of the duct. It is important to note that for all cases the deviation in the pressure distribution is decreased with the turning angle and the maximum radial pressure gradient is occured at 45-deg turning angle. For linear distortion (case 2 and 3) the deviation increases as the distortion increases and the maximum deviation occurs at the duct

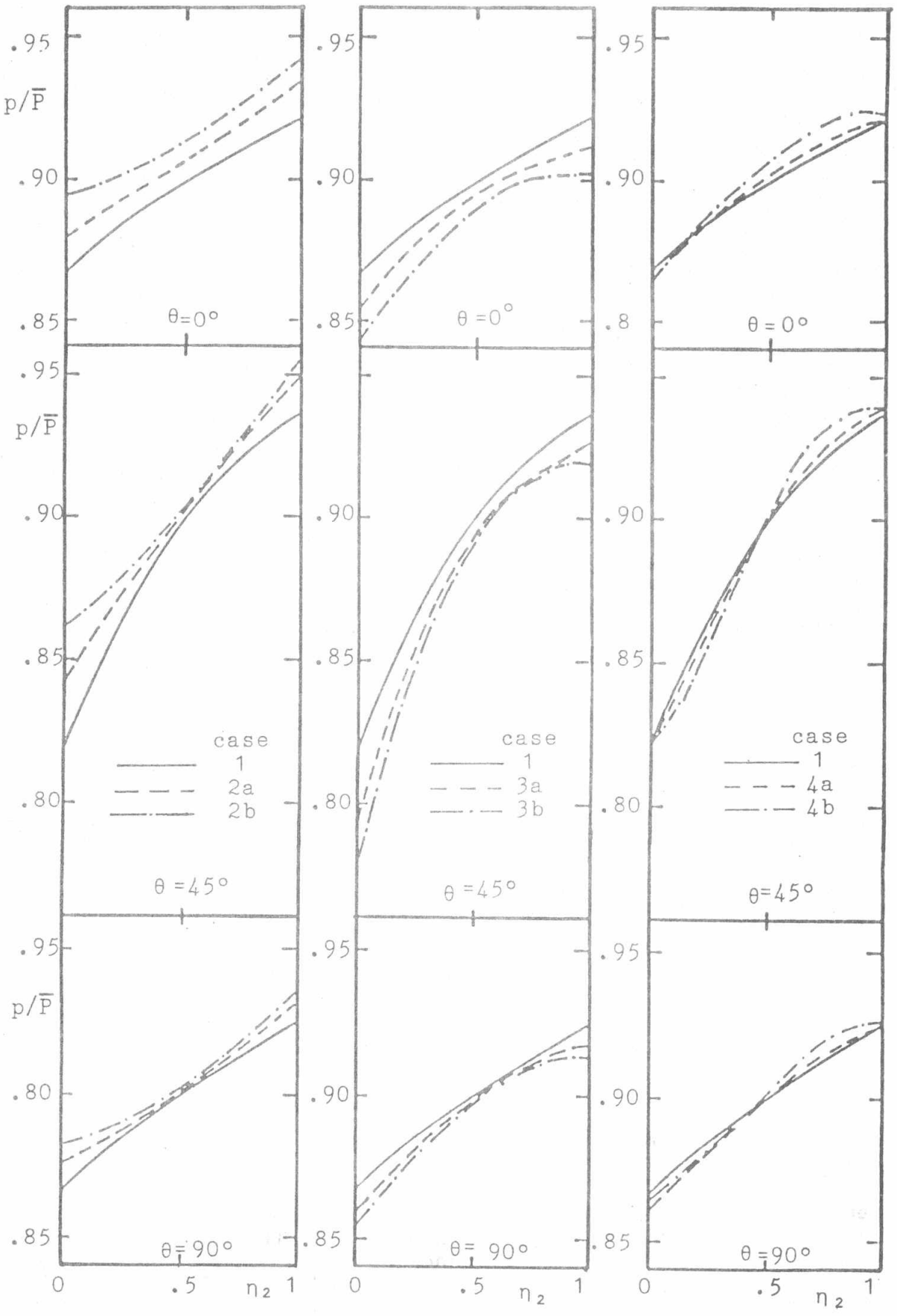

Fig.3 Static pressure distribution in radial direction

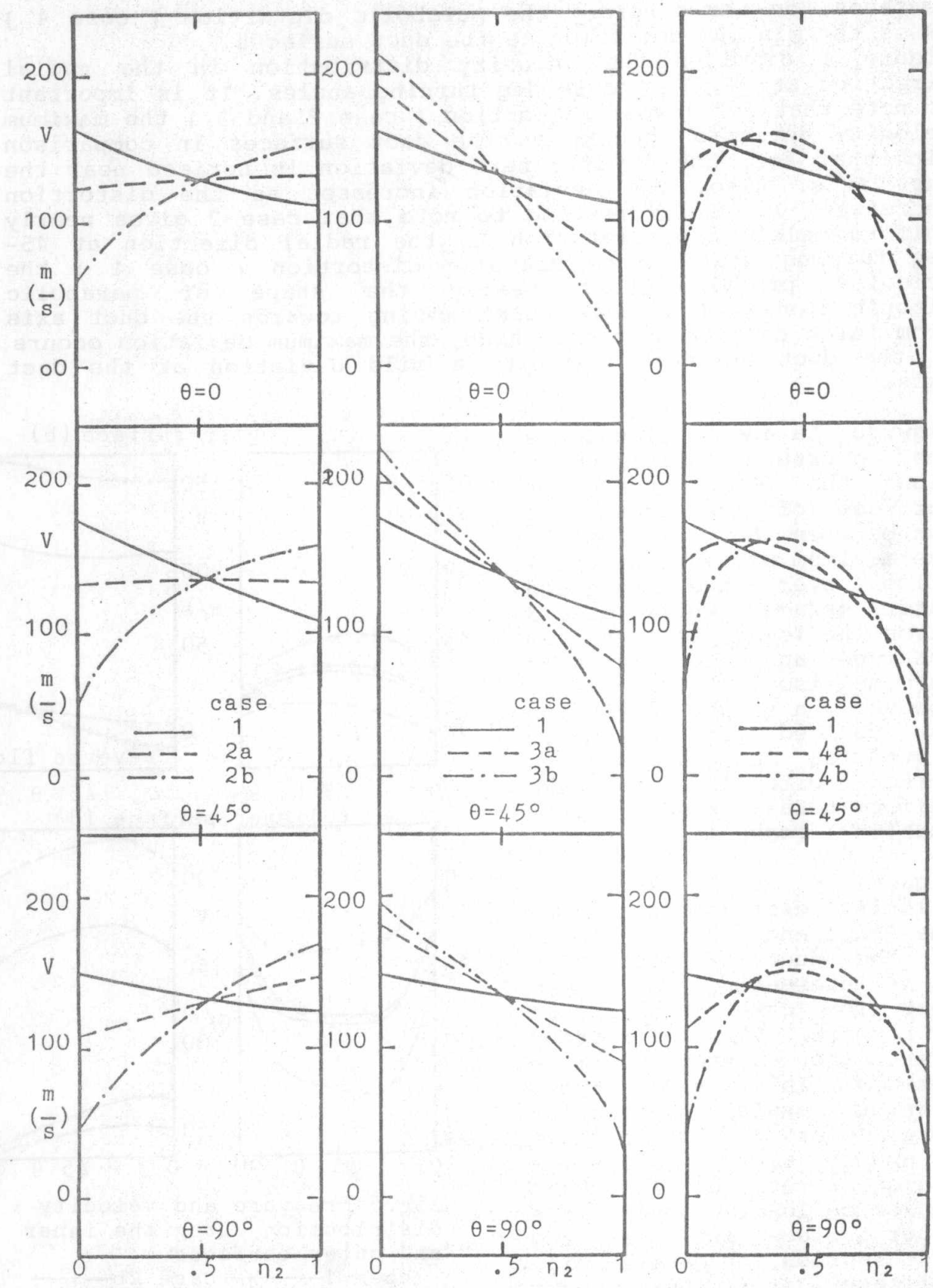

Fig. 4. Velocity distribution in radial direction

surfaces, on the contrary the parabolic distortion (case 4) gives the minimum deviation at the duct surfaces.
Figure 4 displays the velocity distribution in the radial direction at 0-,45- and 90-deg turning angles. It is important to note that for linear distortion (case 2 and 3) the maximum velocity deviation occurs at the duct surfaces in comparison with that for case 1 while zero deviation is noticed near the duct axis. Also, the deviation increases as the distortion increases. It is interesting to note that case 2 gives nearly uniform velocity distribution in the radial direction at 45-deg turning angle. For parabolic distortion (case 4) the velocity profiles take nearly the shape of parabolic distribution with a peak point moving towards the duct axis from inlet to exit sections. Also, the maximum deviation occurs at the duct surfaces but with a mild deviation at the duct axis.

Figures 5a and 5c illustrate the pressure distribution along the inner and outer surfaces of the duct . It can be seen that case 2 gives the maximum pressure distribution over the inner and outer urfaces while case 3 gives the lower pressure over the inner and outer surfaces in comparison with all cases. However , a slight deviation is noticed for parabolic distortion (case 4) in comparison with that for the uniform total pressure distribution (case 1) .

Figures 5b and 5d show the velocity distribution along the inner and outer surfaces of the duct respectively. It is interesting to note that for case 4b a region of reverse flow is formed over the outer surface between inlet and 25-deg turning angle. A slightly more linear distortion(case 2 and 3) can produce a region of reverse flow. This region is located over the inner surface and near the exit section for case 2 while for case 3 it is located over the outer surface and near the inlet section.

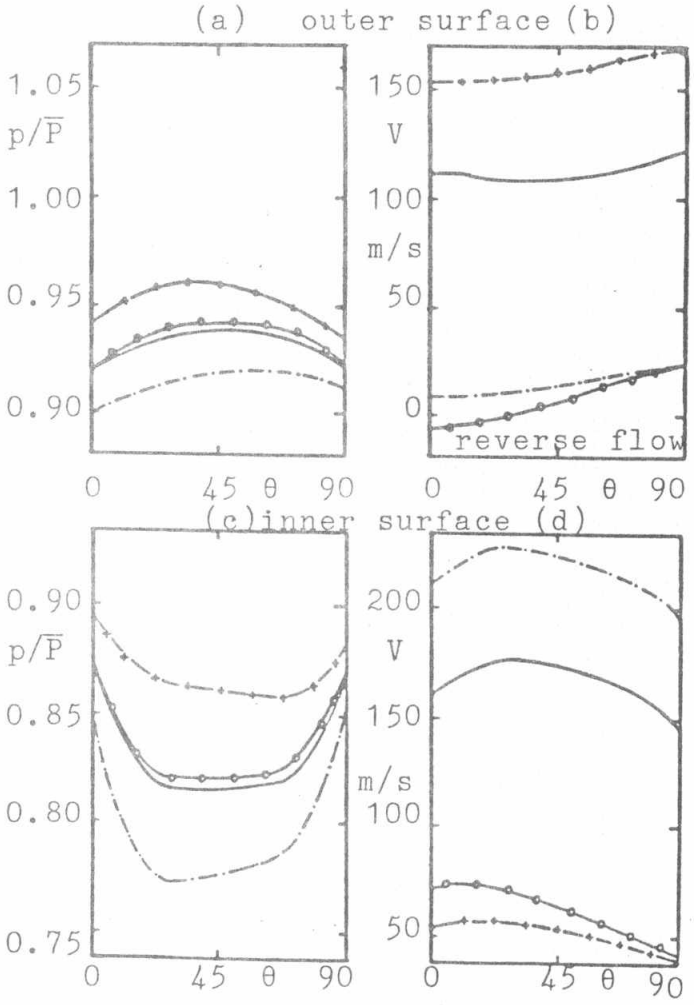

Fig.5 Pressure and velocity distribution along the inner and outer surfaces.
case 1——— case 2b—+—
case 3b—·— case 4b—o—

The maximum deviation in total pressure, static pressure and Mach number in comparison with those for case of uniform total pressure distribution (case 1) are given in Table 1.

Table 1 Maximum % Deviation

Flow property	case 2		case 3		case 4	
	a	b	a	b	a	b
Total pressure	5.0	9.5	5.0	9.5	5.0	9.5
Static pressure	3.2	5.8	3.3	5.2	0.4	0.7
Mach number	23	47	33	70	45	100

It can be seen that the deviation in static pressures is small in comparison with Mach numbers. The parabolic distortion (case 4) gives the minimum deviation in static pressure compared with linear distortion (cases 2 and 3) while it gives a pronounced deviation in Mach number. The results of the static pressure are resonable but those of velocity are less acceptable, a direct consequence of the uniform inlet total pressure assumption.

Conclusions

Numerical solutions for an inviscid, compressible flow in a two-dimensional 90-deg curved duct with different cases of inlet total pressure distortion are obtained. The validity of the uniform total pressure assumption for the cases of inlet total pressure distortion is tested. The assumption of uniform inlet total pressure results in a reasonable static pressure distribution, but if accurate velocity distributions are required, the actual inlet total pressure distribution must be used.

References

1. COLPIN, J. "Propagation of Inlet Flow Distortion Through an Axial Compressor Stage", ASME, Paper No. 78-GT-34, 1978.
2. BILLET, G., LAVAL, P. and CHEVALIER, P., " Response of an Axial Compressor to Distorted Inlet Flow ", Computional Methods in Turbomachinery, I Mech E Conference Publications 1984-3, London, Paper C75/84, pp.211-220, April 1984.
3. ABDELRAHMAN, M., M. "Development of a Short Compution Time Implicit Method for Computing Transonic Flows with Strong Shock Waves", 6th International Symposium on Air Breathing Engines (ISABE), Paris, 6-11 June 1983.
4. SALEM, G., B. and ABDELRAHMAN, M. M., "Inviscid Solution for the Compressible Flow in Curved Ducts Using Micro-Computer" Scientific Engineering Bulletin, Faculty of Engineering, Cairo University, Number 3, 1986.